GEO-DEEP 9300: Introduction to receiver functions and discontinuities

Valerie Maupin

Many figures from IRIS training school lecture from Anne Sheehan (2006)
and from Stein and Wysession:

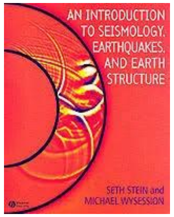

Body wave and surface wave tomography give smooth profiles

Phase velocity of Rayleigh wave as a function of plate age in the Pacific Ocean

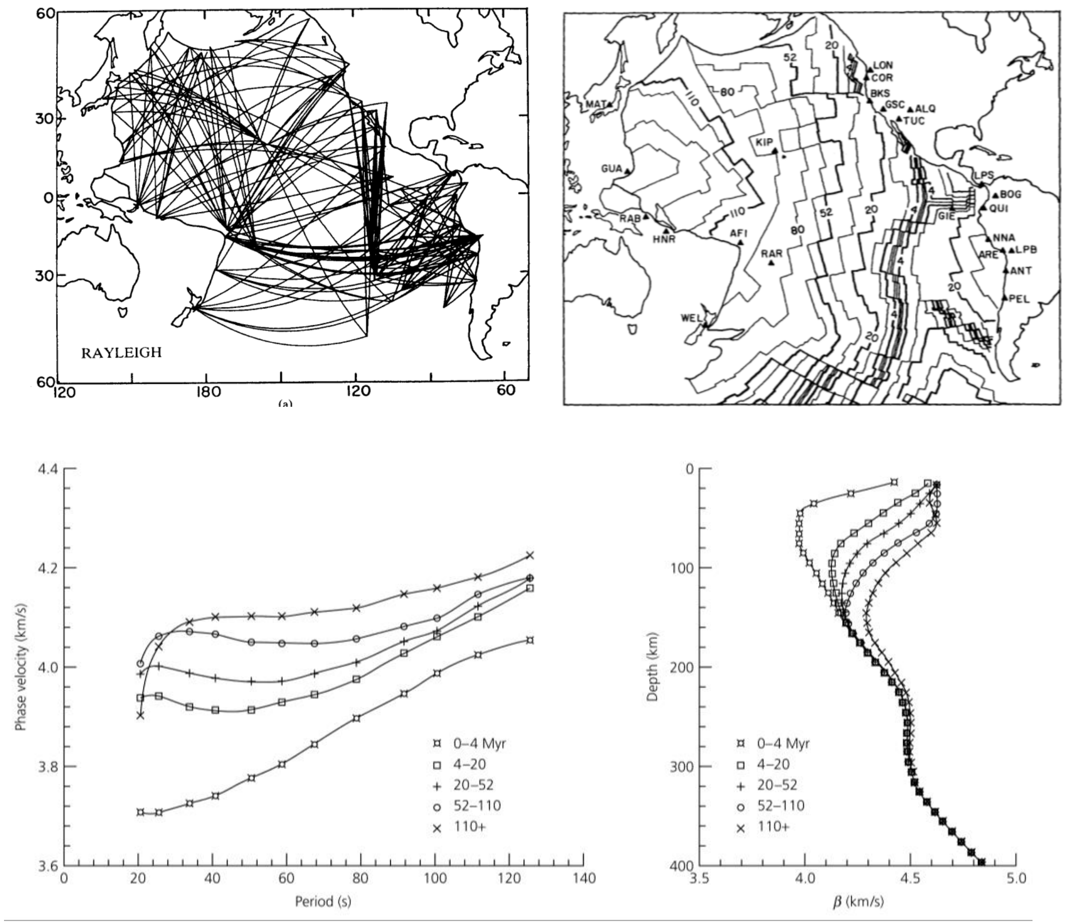

Nishimura and Forsyth, (1989)

Can we detect discontinuities with seismic waves?

What does discontinuities do to the seismic waves?

Reflection, transmission and conversion

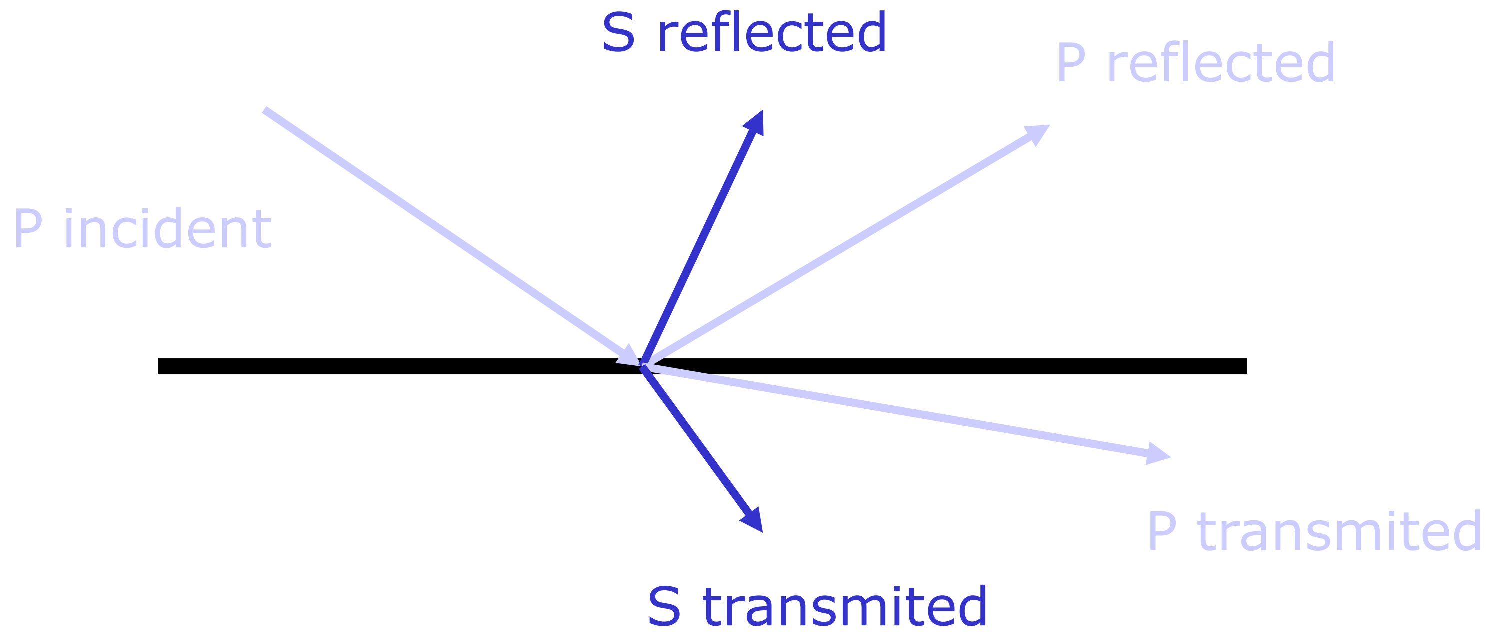

UNIVERSITY OF OSLO

Snell’s law

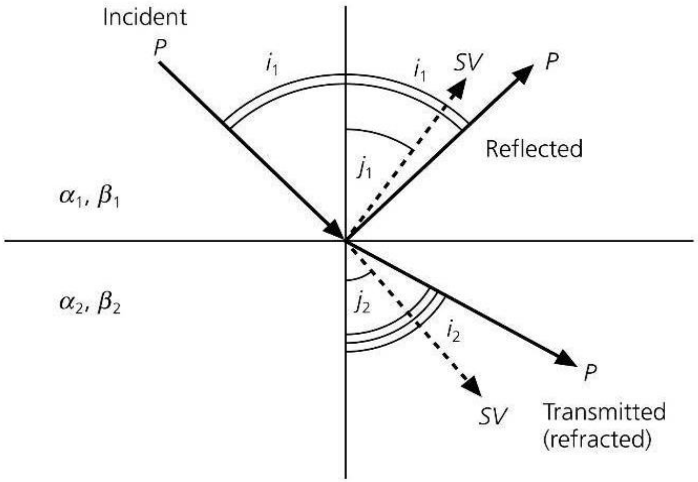

Goal: detect interfaces in the subsurface

Reflection seismics:
OK, but not for the lithosphere

Figure 1.1-5: Demonstration of the seismic reflection method.

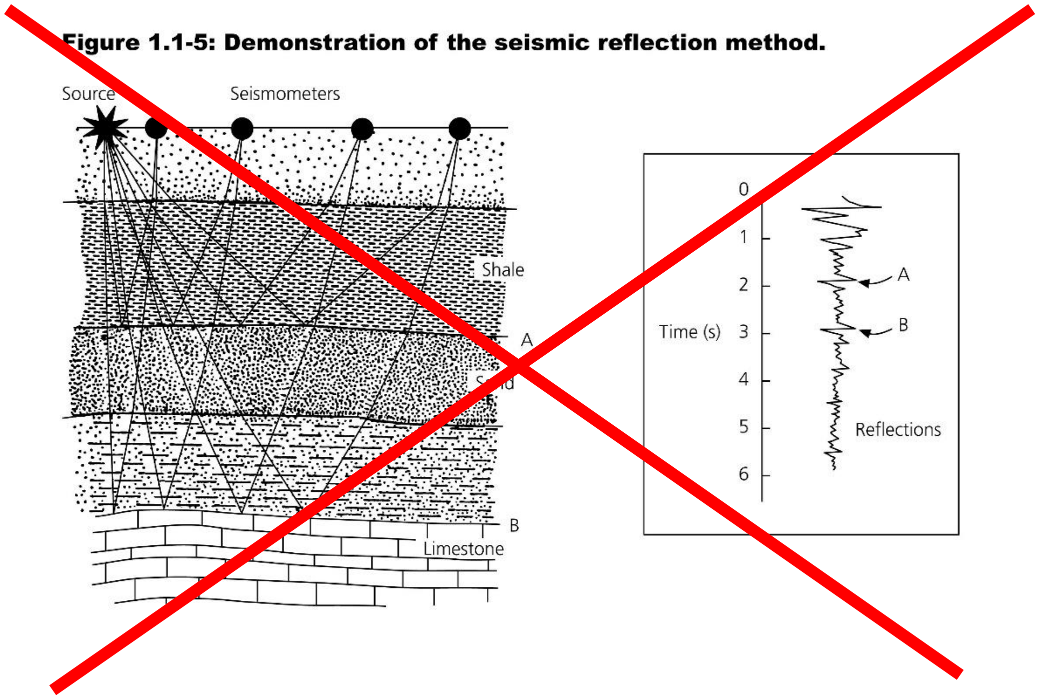

Examples of converted/reflected waves used for mantle studies

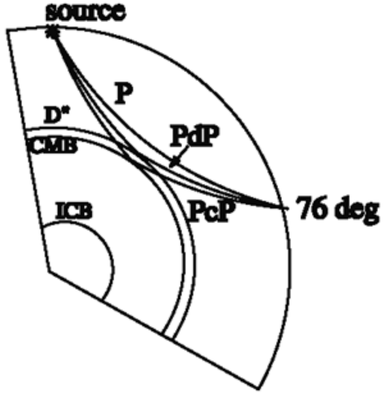

Reflected P

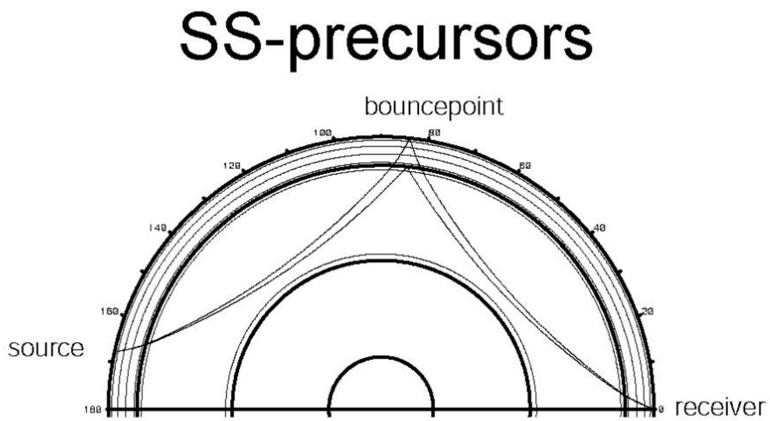

Reflected S

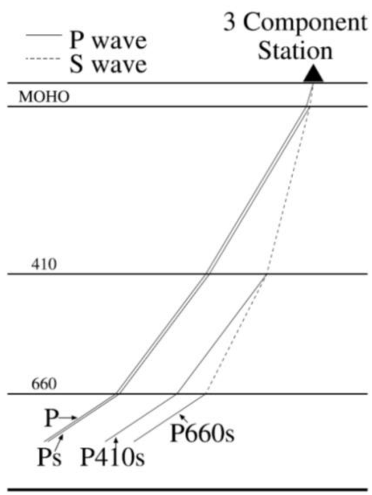

Converted P to S

Minor waves relative to a major one

Receiver functions

Figure 1.1-3: Example of seismogram, showing accompanying ray paths.

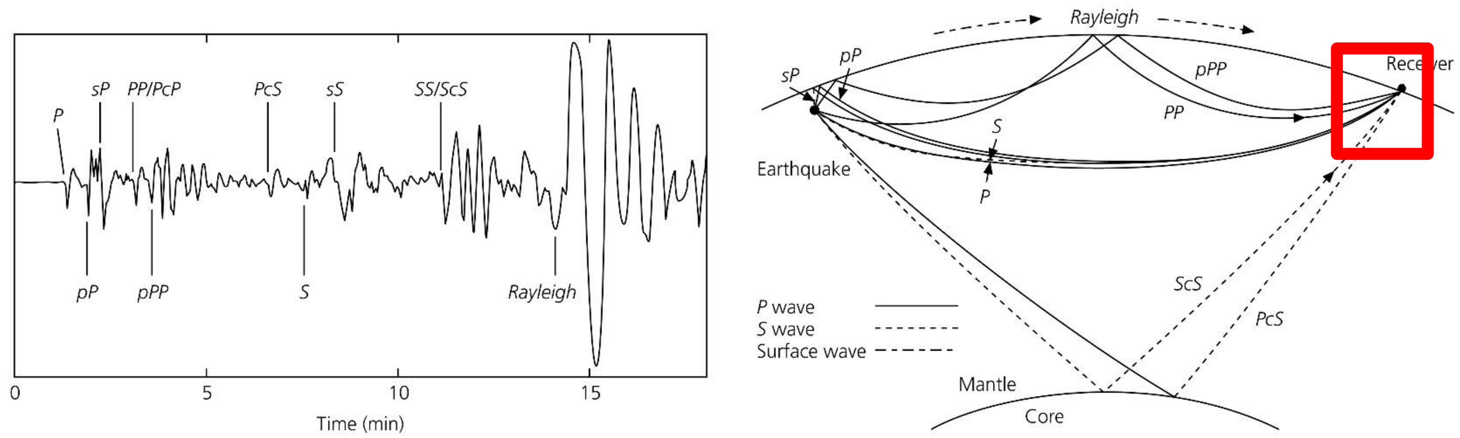

UNIVERSITY OF OSLO

Receiver functions

- Principle of P-receiver function
- P- and S-receiver functions
- Applications for Moho and LAB depth
- Applications for 410 and 660 discontinuity

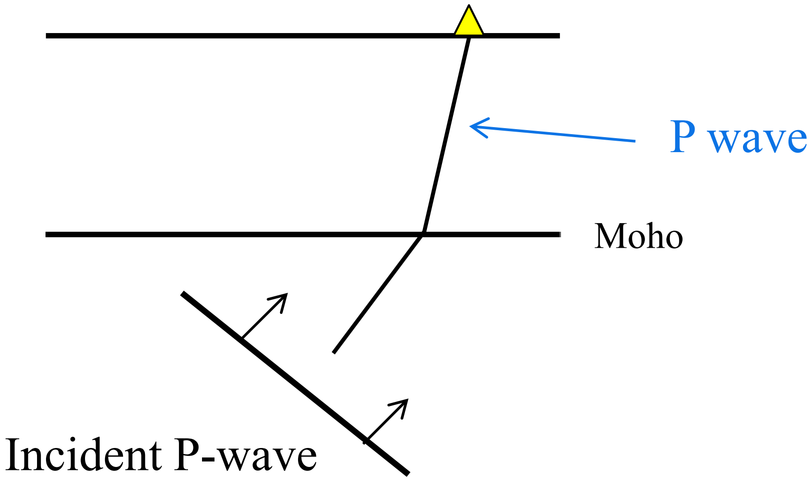
P wave
Moho
Incident P-wave

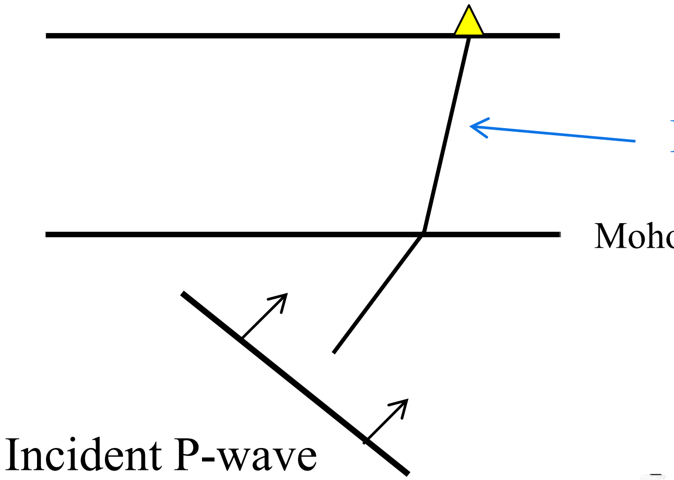
Refracted P wave.
Moho
Incident P-wave

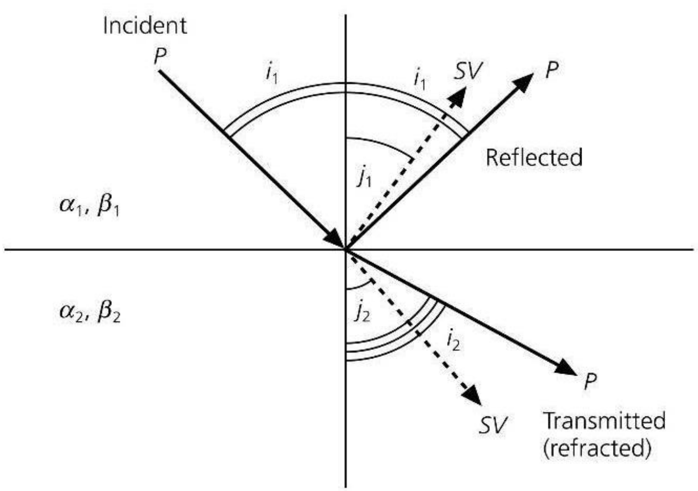
Incident
P
i_1
i_1
SV
P
Reflected
j_1
α_1, β_1
α_2, β_2
j_2
i_2
P
SV
Transmitted
(refracted)

Snell's law

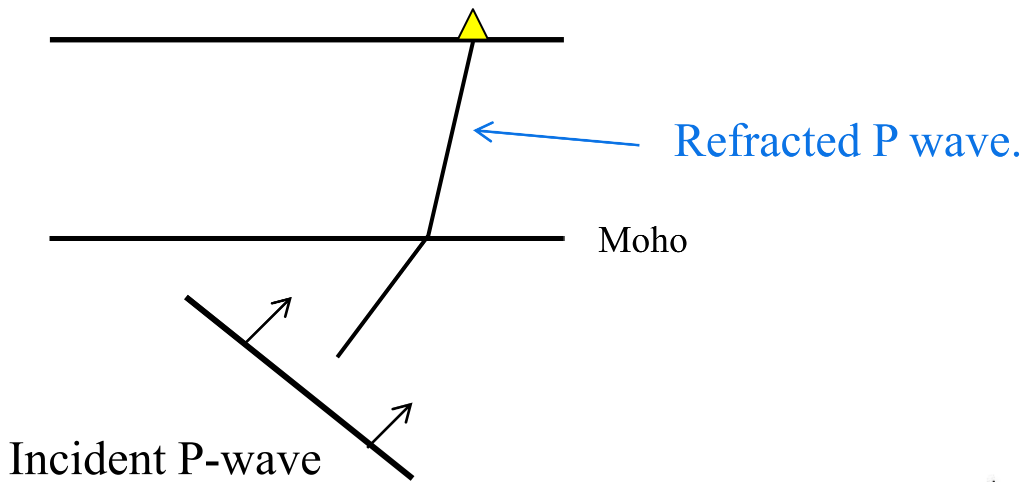
Refracted P wave.
Moho
Incident P-wave

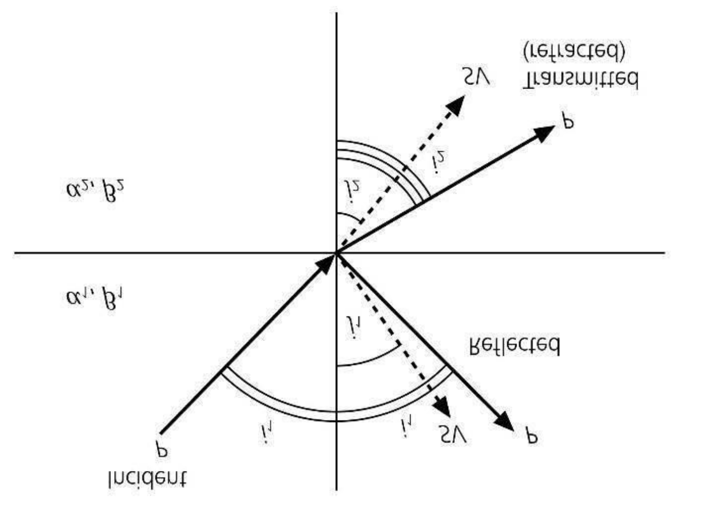
Transmitted
(refracted)
SV
P
Reflected
P
SV
Incident
P

Snell’s law

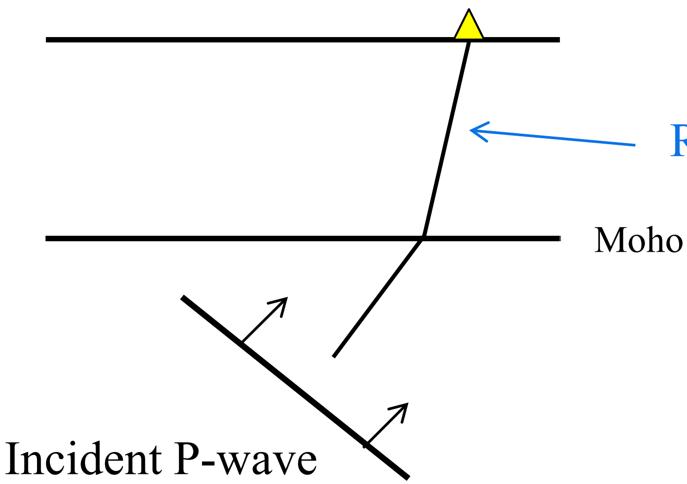

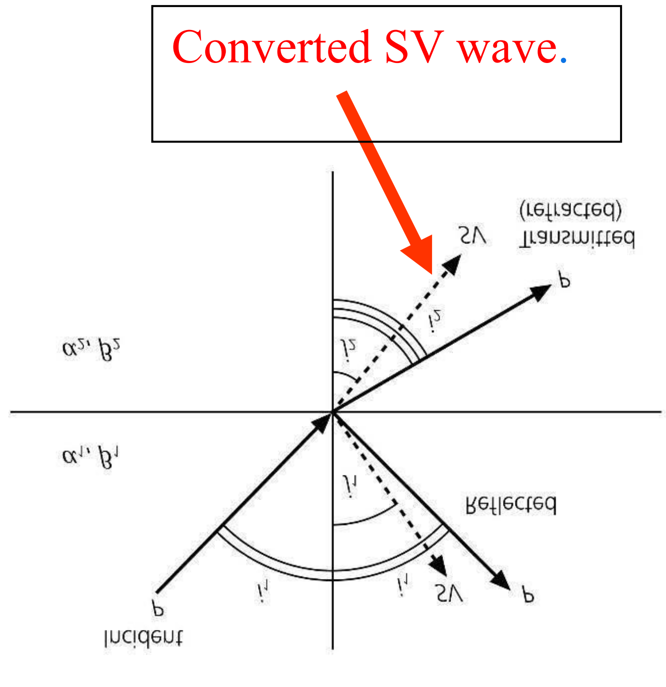

Snell's law

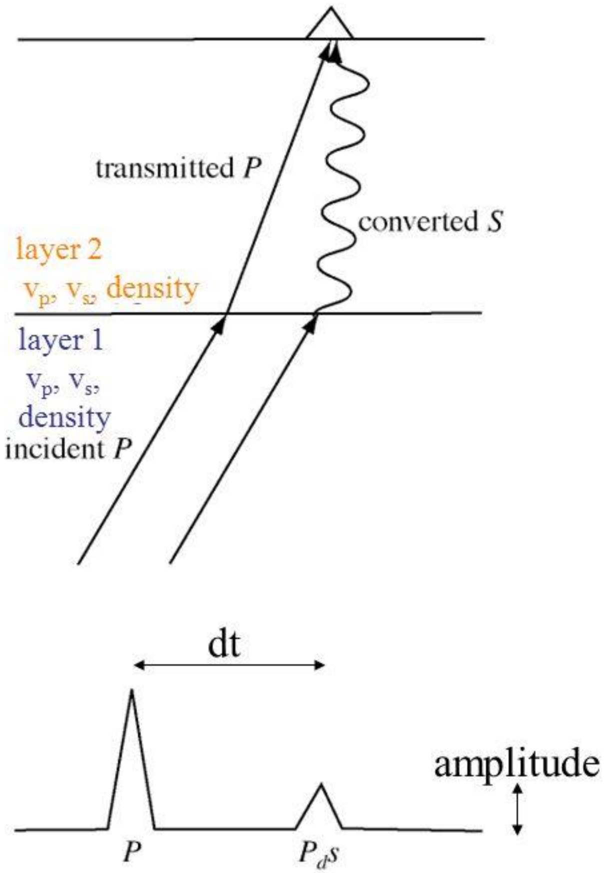

converted pulse:

delay time dt depends on depth of interface and v_p, v_s of top layer

amplitude depends on velocity contrast (mostly) and density contrast (weakly) at the interface

converted arrival:
"+" bump = bottom slow, top fast
"-" bump = bottom fast, top slow

University of Oslo

Figure 6.3-7: Diagram of the receiver function approach.

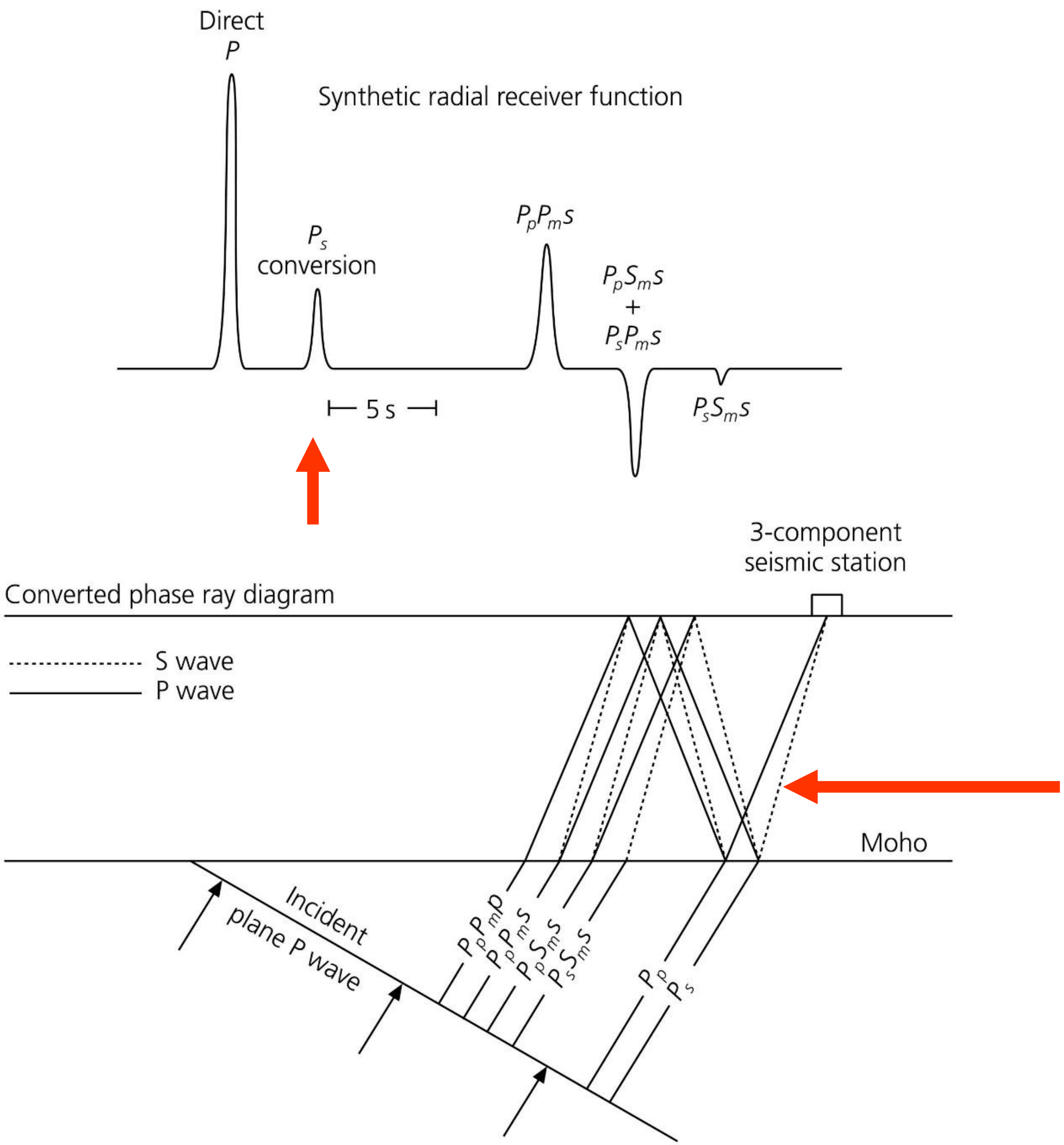

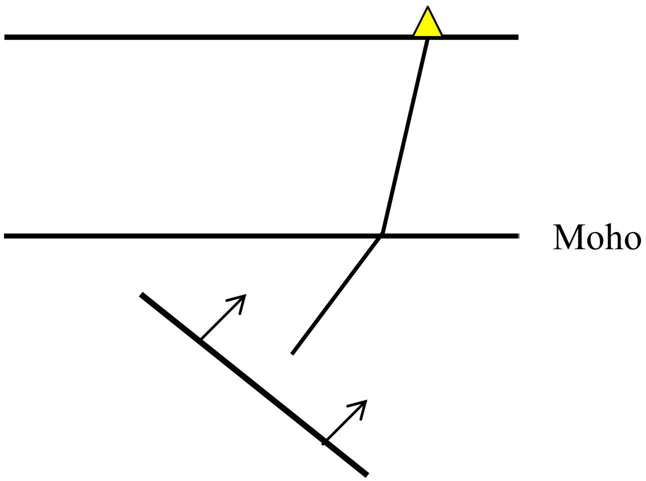

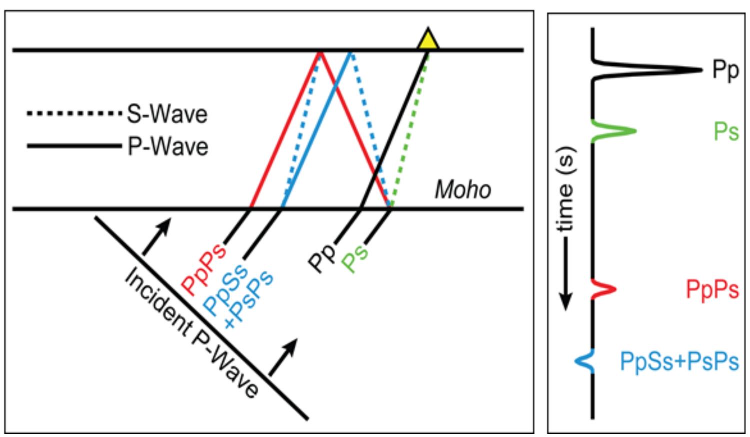

Reverberations may interfere with first arrival

UNIVERSITY OF OSLO

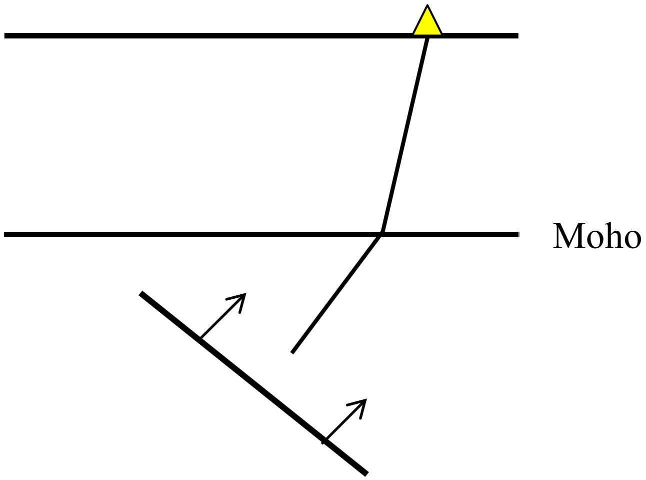

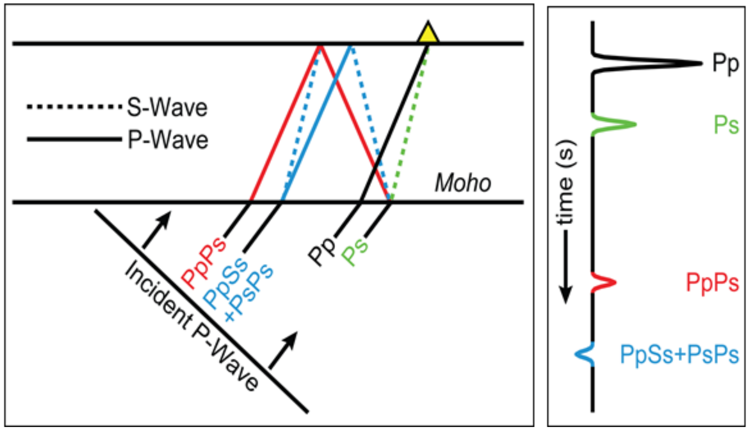

Sediments may bring additional phases

A single receiver function - hard to interpret

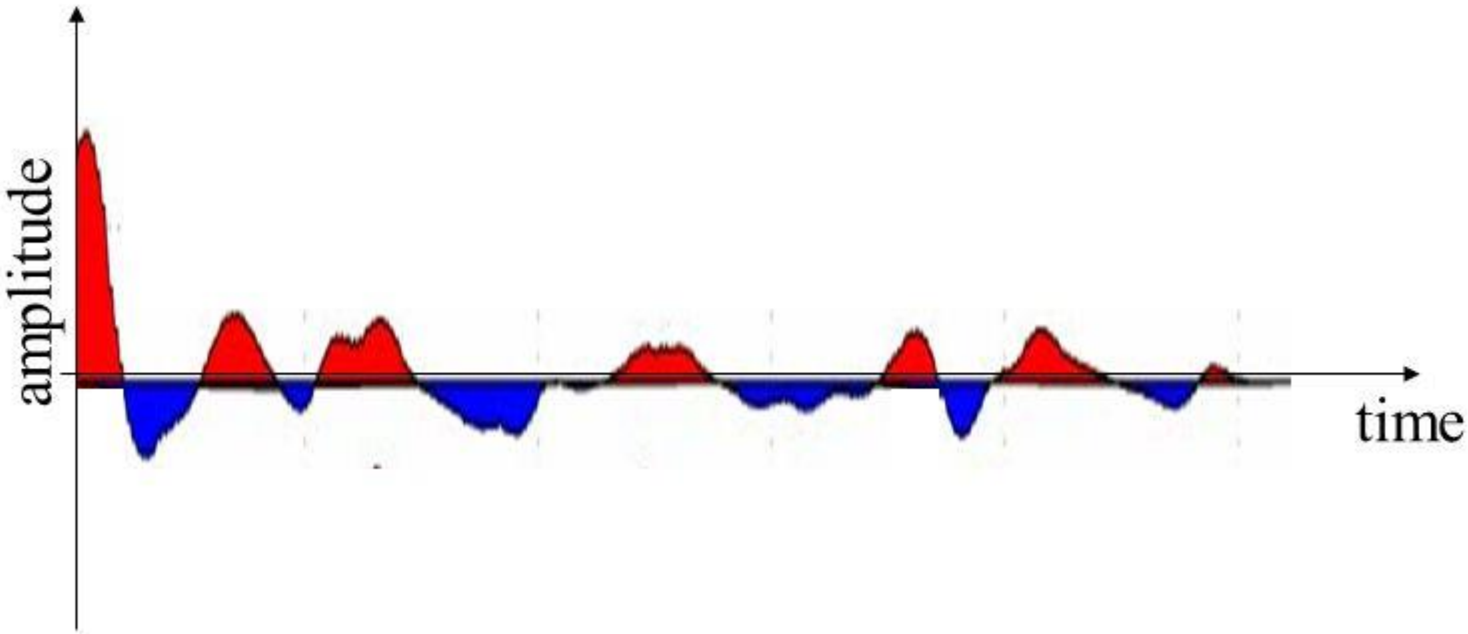

one receiver function per earthquake
-function of slowness (incidence angle)
-function of backazimuth (unless flat layered isotropic case)

unfortunately, incident P is not a nice simple bump:

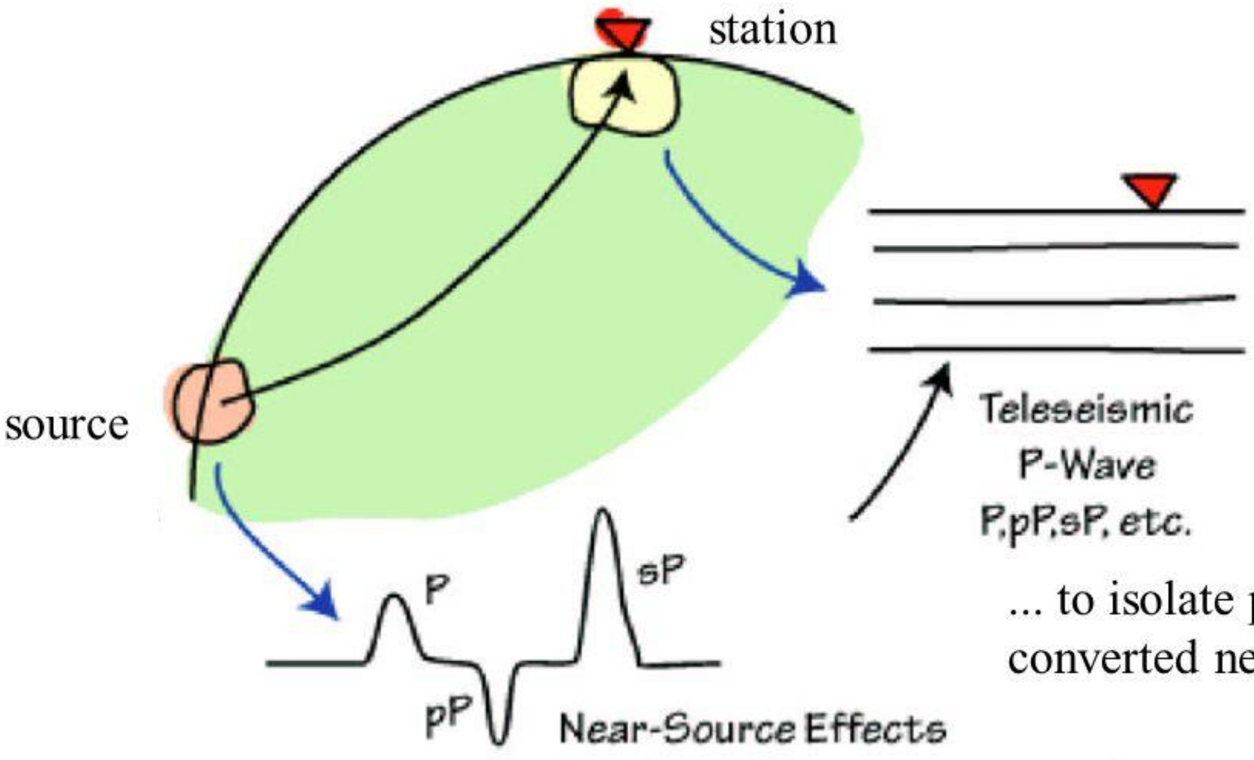

... to isolate phases
converted near station

need to remove these bits ...

Deconvolution of the source (earthquake) function

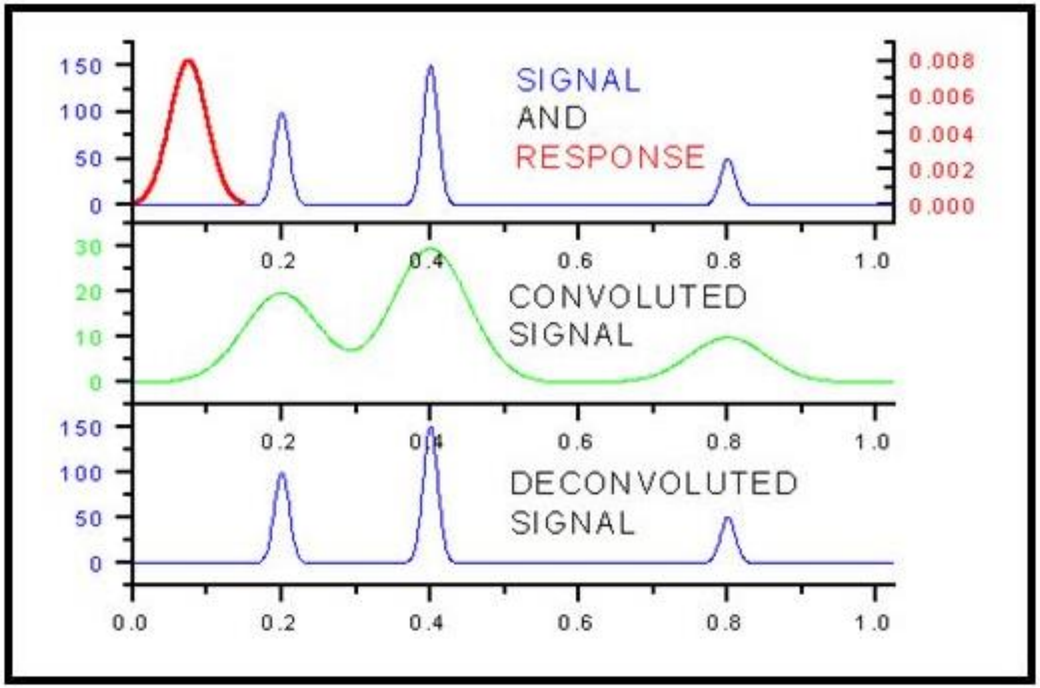

UNIVERSITY OF OSLO

Stack of events: average over azimuth

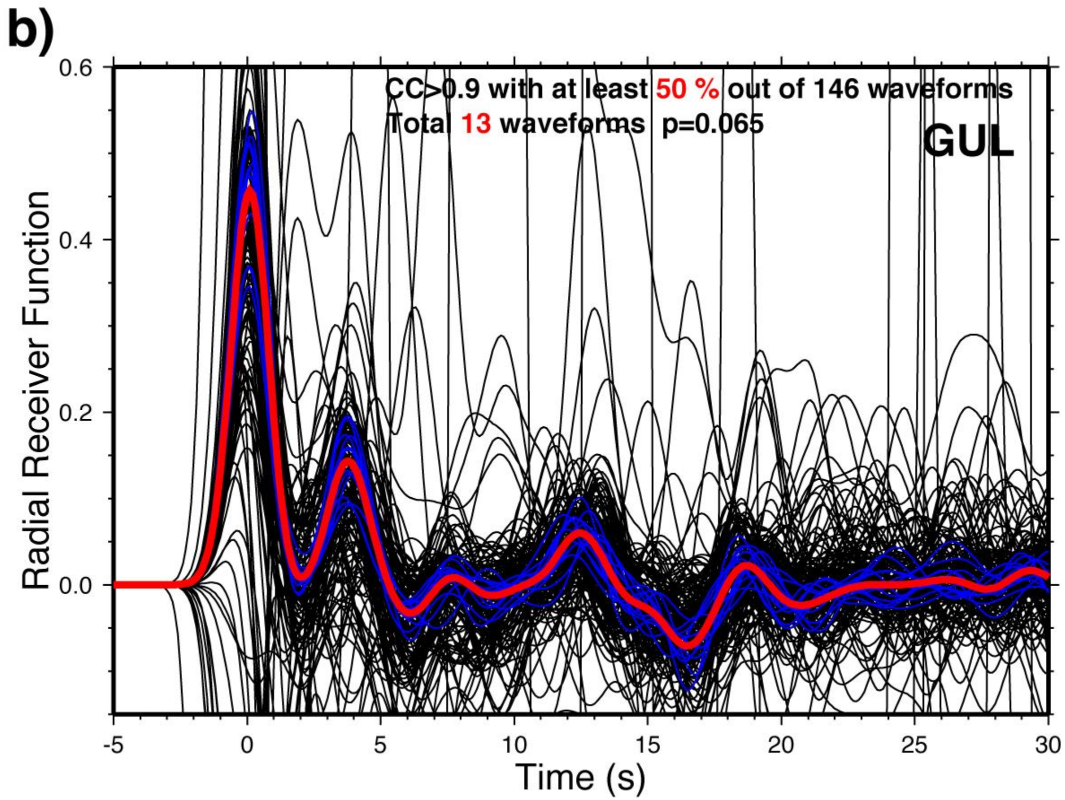

from Tkalcic et al., 2010

Can RF show a sharp lithosphere-asthenosphere boundary?

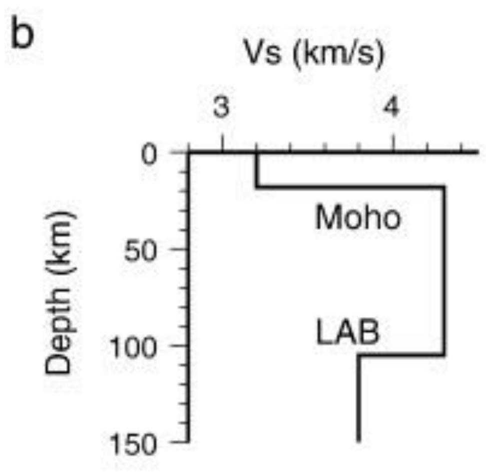

Kind et al.., 2012

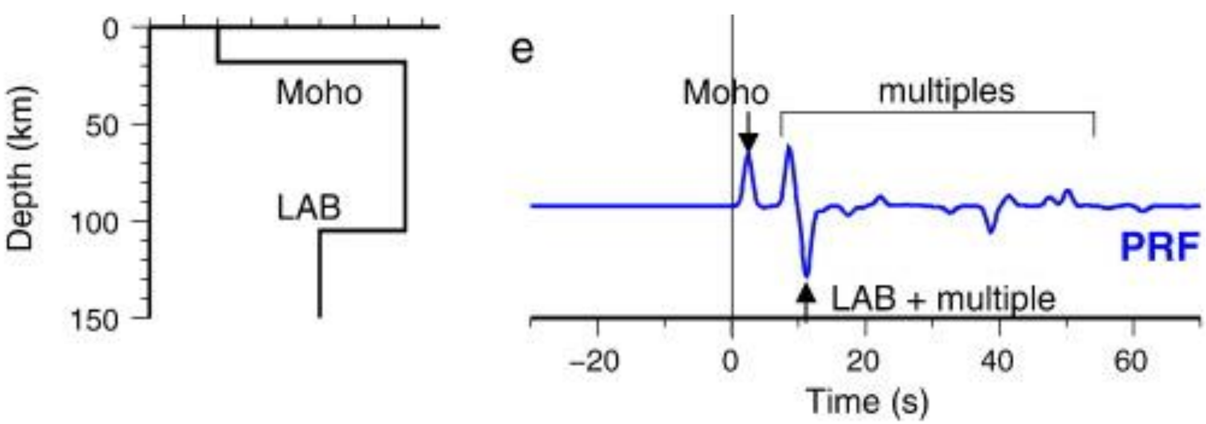

Kind et al.., 2012

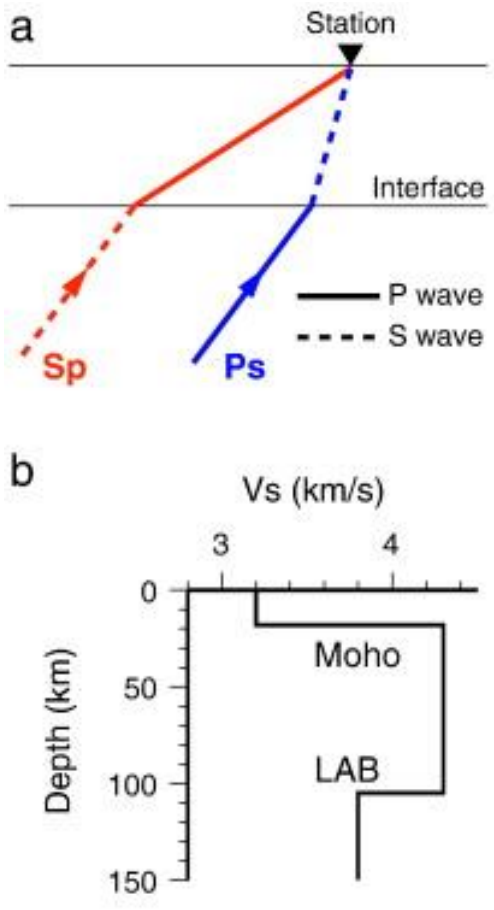

P-receiver function
and
S-receiver function

Kind et al.., 2012

UNIVERSITY OF OSLO

Snell's law for incident P and incident SV

Figure 2.5-5: Transmitted and reflected waves for incident *P* and *SV* waves.

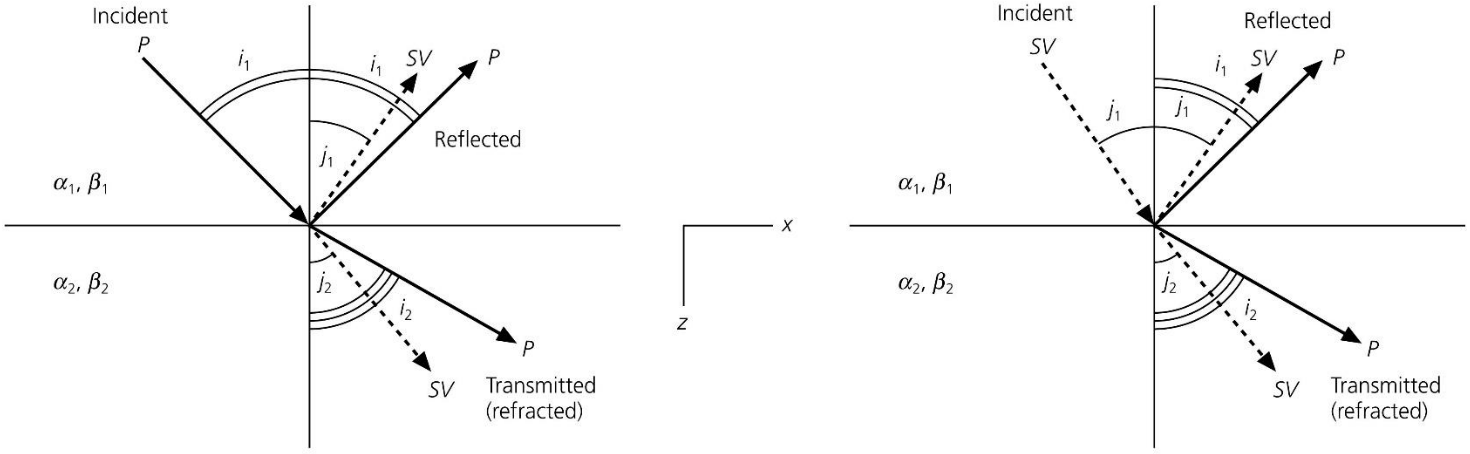

UNIVERSITY OF OSLO

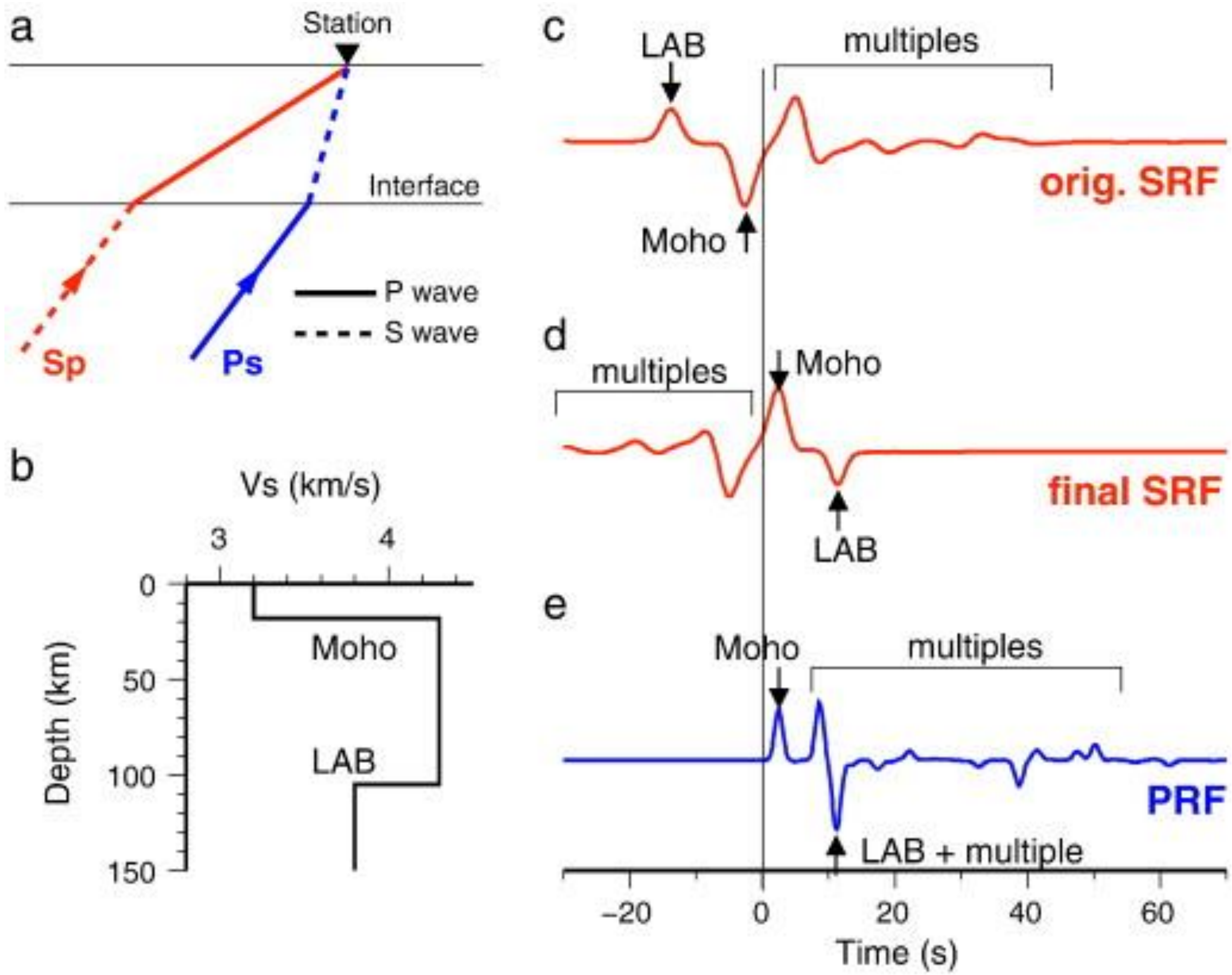

Kind et al.., 2012

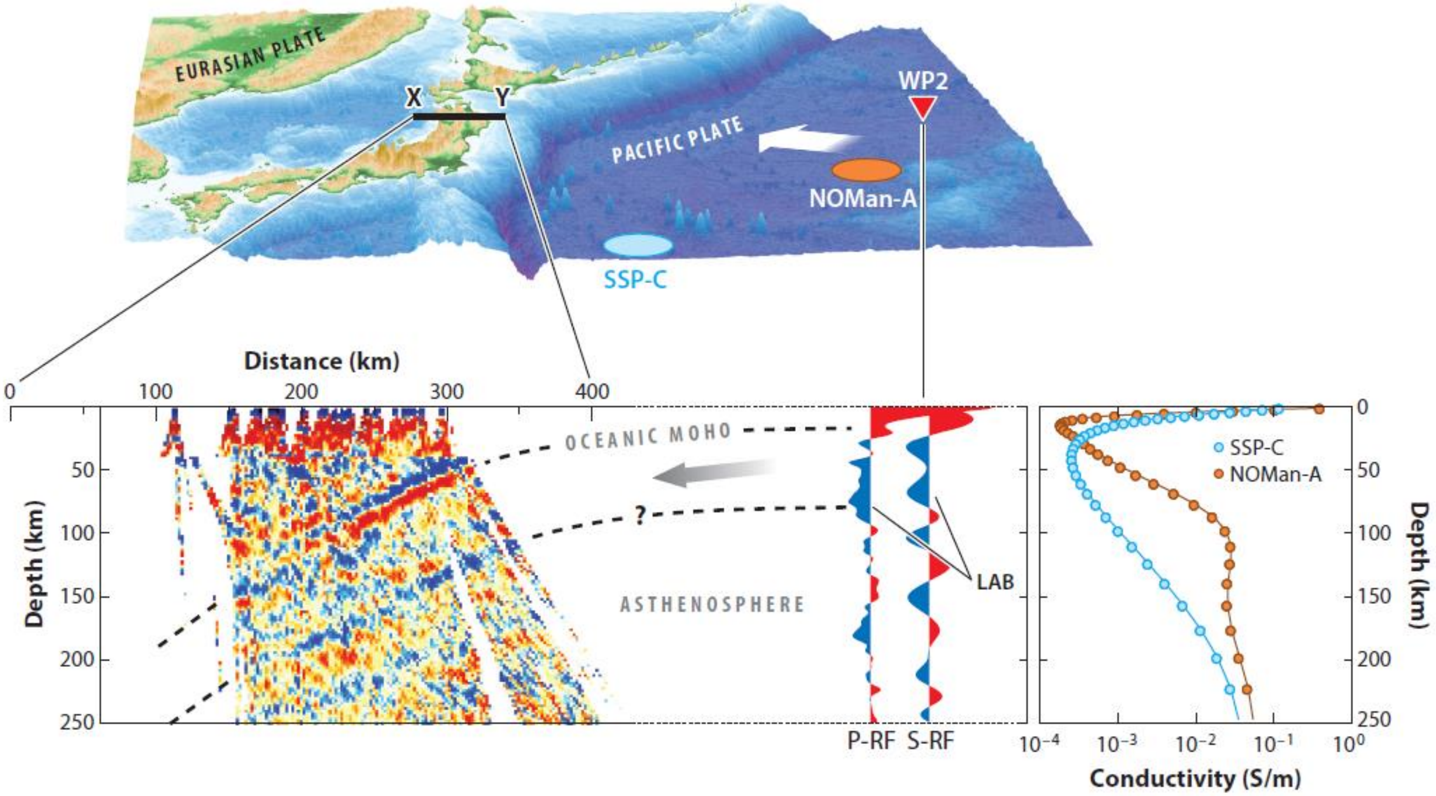

Figure 11

Lithosphere–asthenosphere system at a subduction zone: Shown are a P-RF image using dense land seismic data of Hi-net from Japan and a P-RF and S-RF image for the seafloor borehole station WP2, adapted from Kawakatsu et al. (2009). Also shown are the regional electrical conductivity profiles in two areas, NOMan-A and SSP-C; these data are from Baba et al. (2013). Abbreviations: LAB, lithosphere–asthenosphere boundary; NOMan, Normal Oceanic Mantle Project; P-RF, P-receiver function; S-RF, S-receiver function; SSP, Stagnant Slab Project.

Kawakatsu and Utada., 2017

Detection of the sharpness of the discontinuity

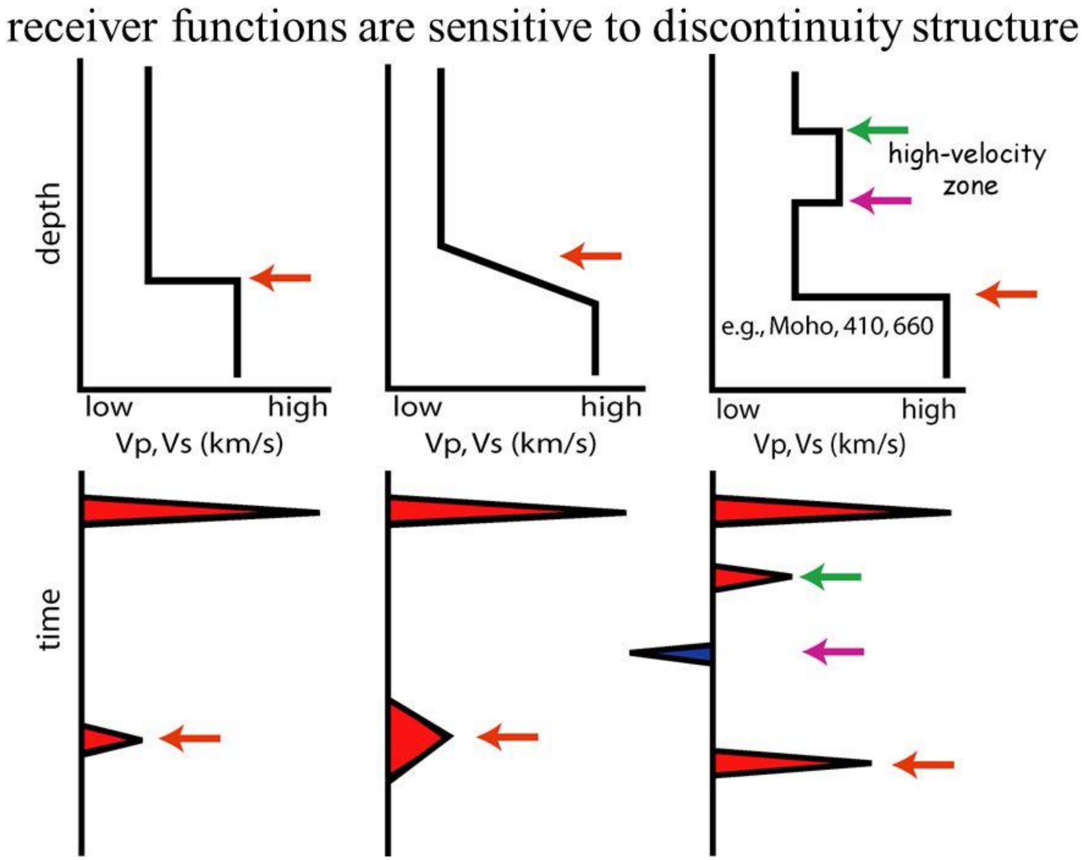

Thickness of interface

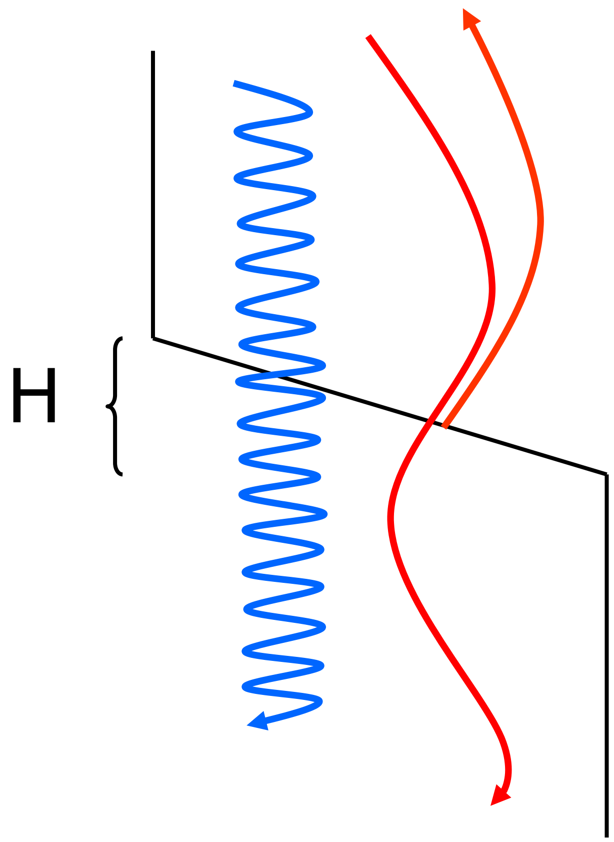

Long wavelengths (>>H)
see an interface

Short wavelengths (<<H)
see a gradient

Detection of the sharpness of the LAB

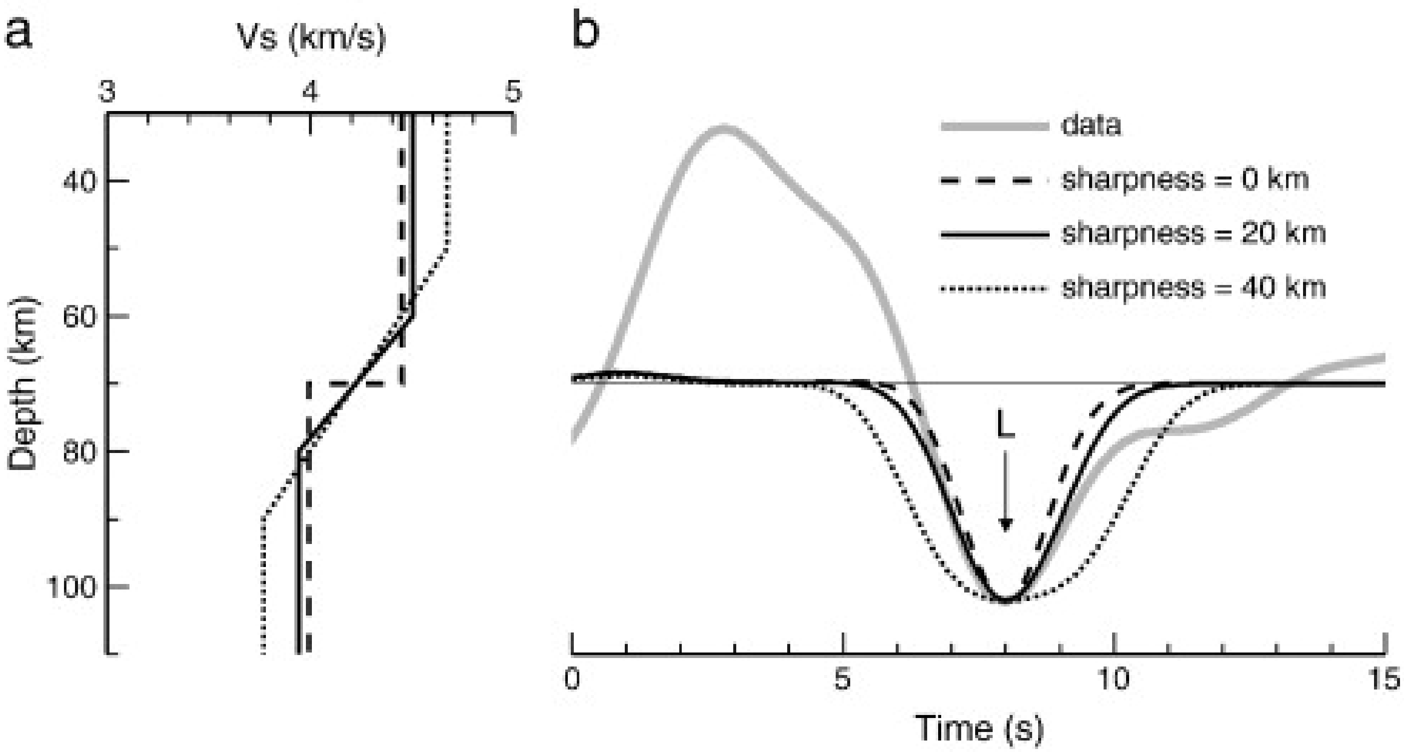

Kind et al.., 2012

Gradient of the LAB

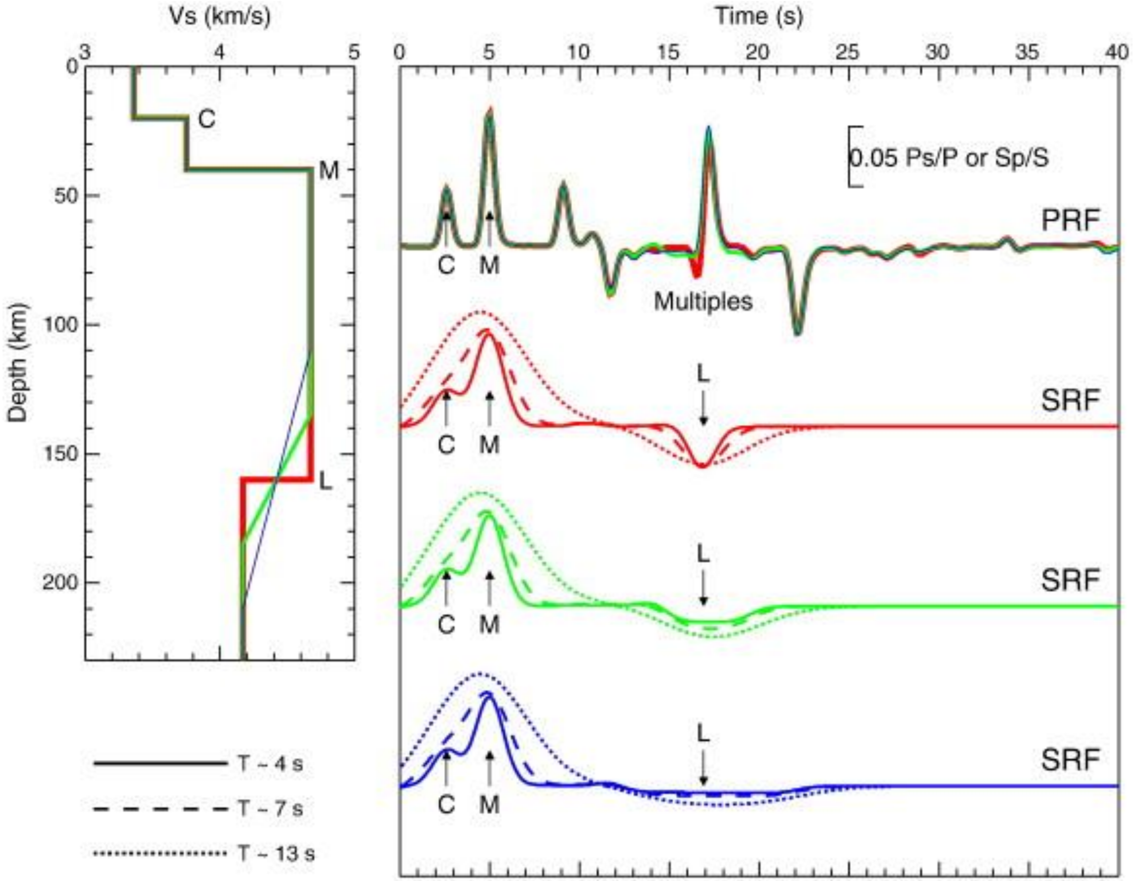

Kind et al.., 2012

UNIVERSITY OF OSLO

LAB or MLD?

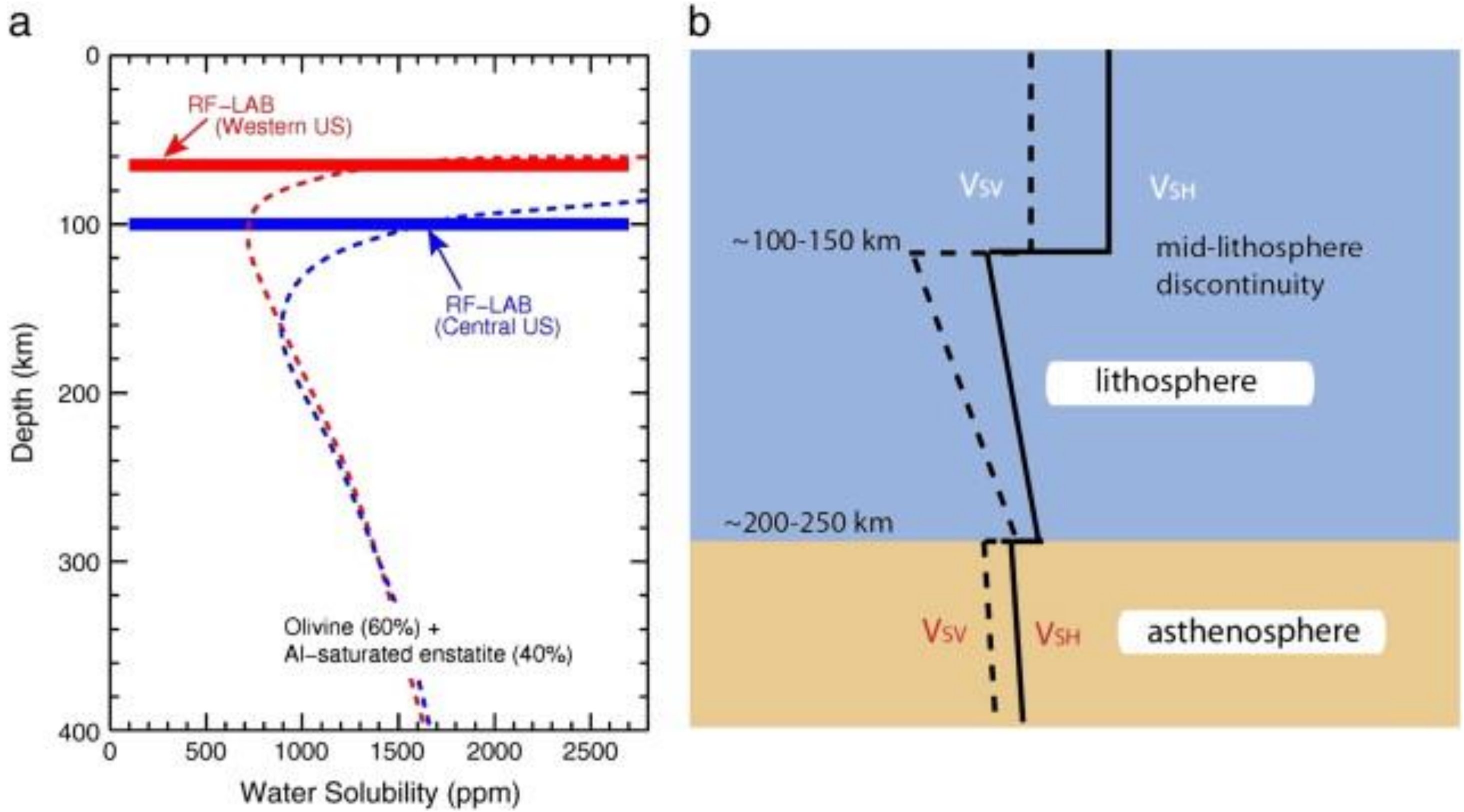

Kind et al.., 2012

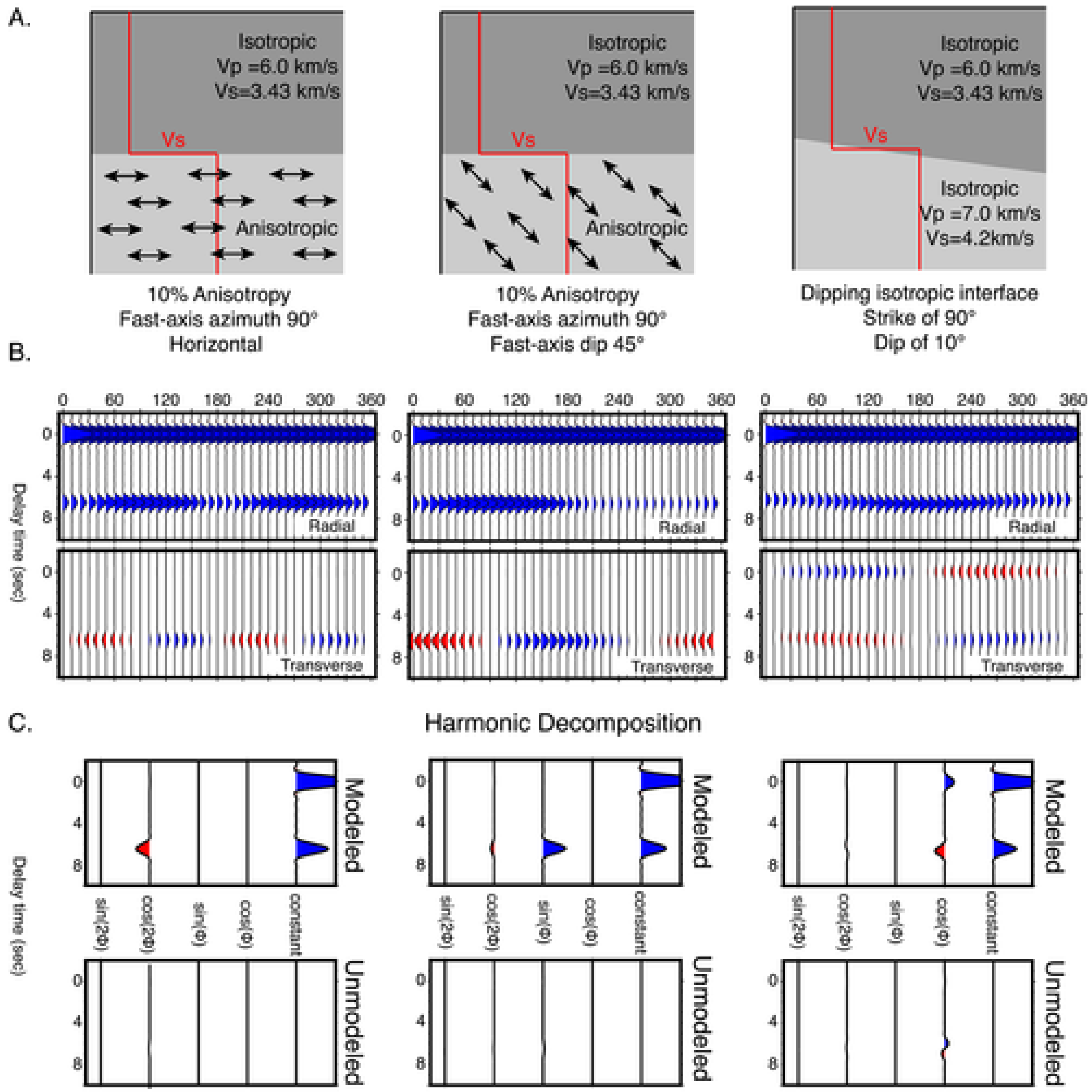

Ford et al.., 2016

RFs:

unique constraints to characterize the LAB

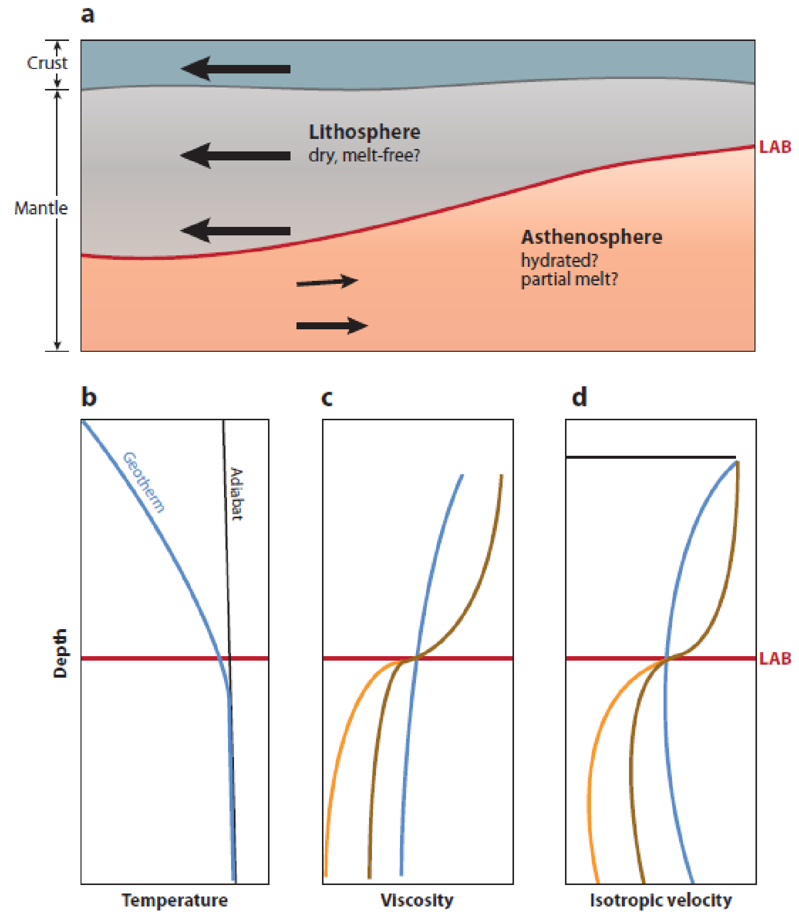

Figure 1

Schematic models of lithosphere-asthenosphere boundary (LAB) properties. (*a*) Depth profile through the lithosphere and asthenosphere. Arrows show the motion of a coherent lithospheric layer over a deforming asthenosphere. (*b*) Temperature as a function of depth. In the absence of other factors, the lithosphere would correspond to the cold thermal boundary layer represented by subadiabatic temperatures. (*c*) Mantle viscosity for three cases. Blue: the geotherm in panel *b*. Brown: the geotherm superimposed on a compositional difference at the LAB (dry lithosphere over hydrated asthenosphere). Orange: the latter case plus partial melt in the asthenosphere. (*d*) Isotropic shear velocity corresponding to the three cases in panel *c*. The black line schematically illustrates the velocity increase from the crust to the mantle.

Receiver functions for 410 and 660 discontinuities

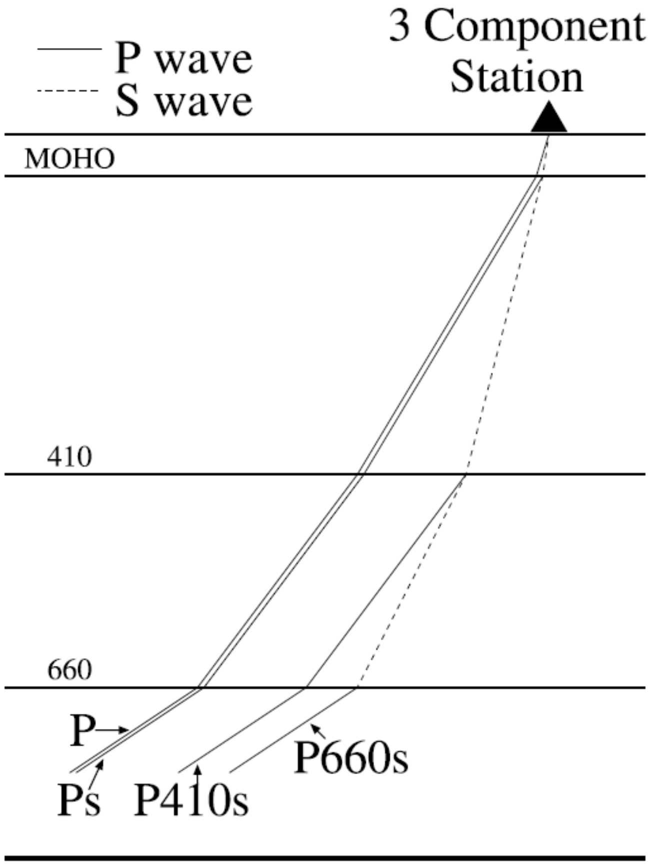

after Andrews and Deuss 2008

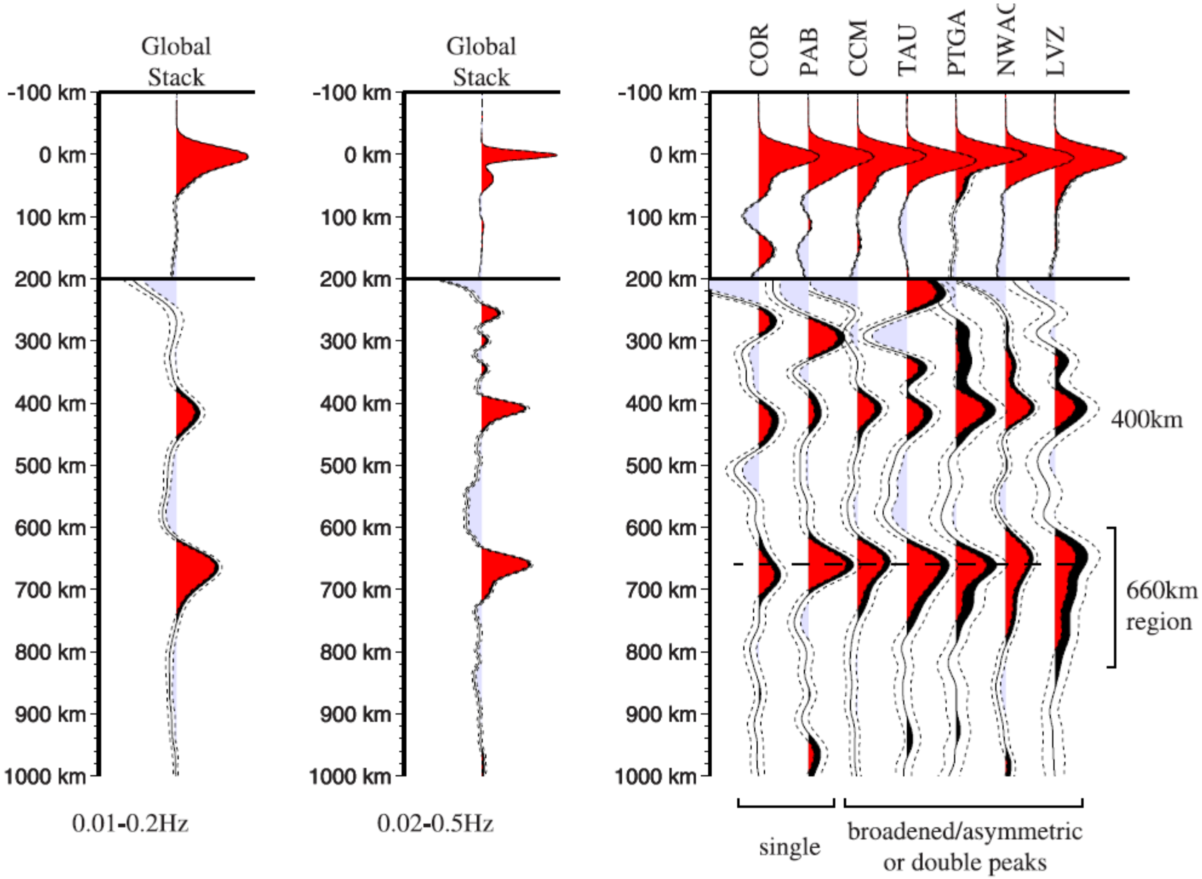

after Andrews and Deuss 2008

Discontinuity variation at subduction zones

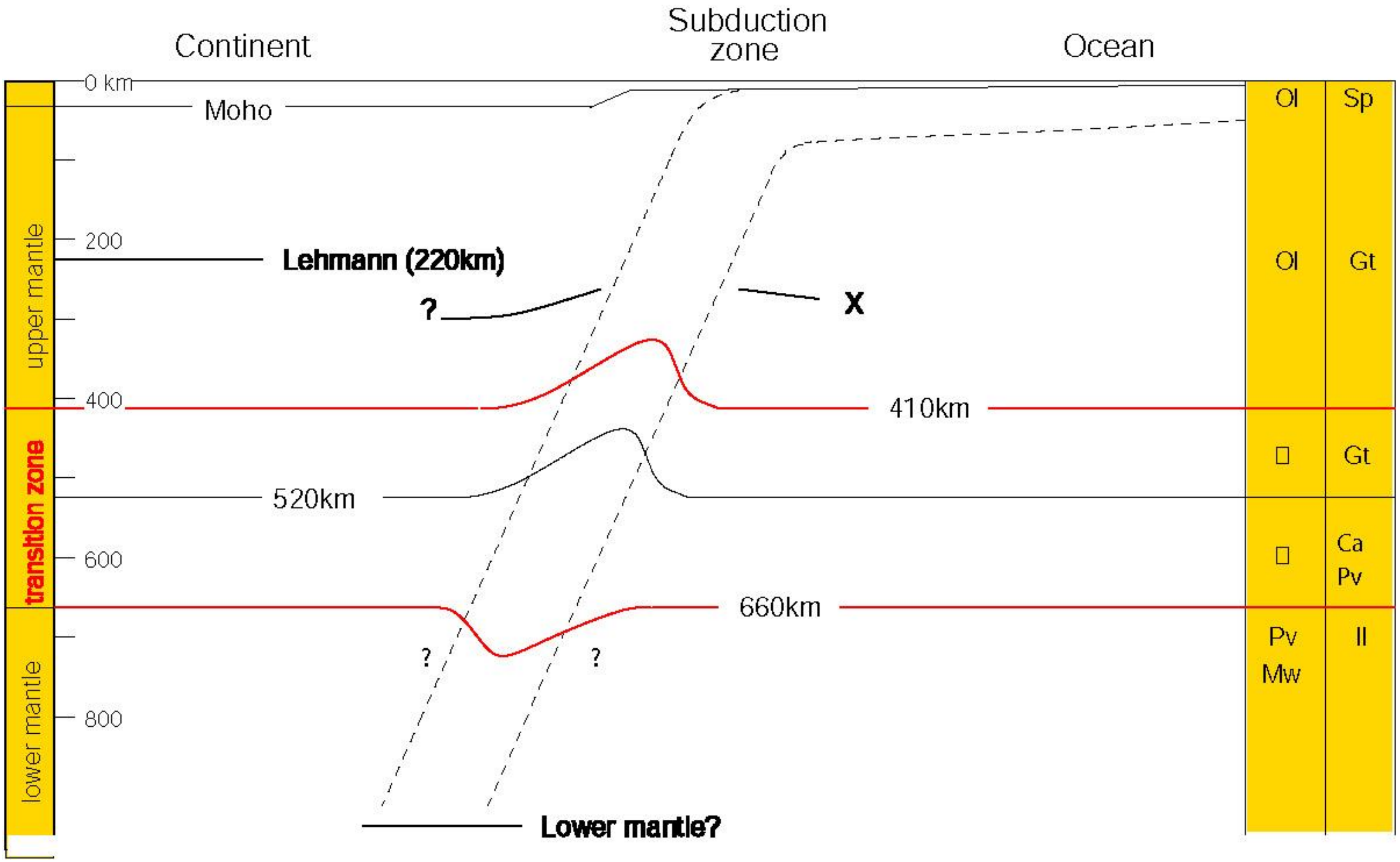

From A. Deuss

UNIVERSITY OF OSLO

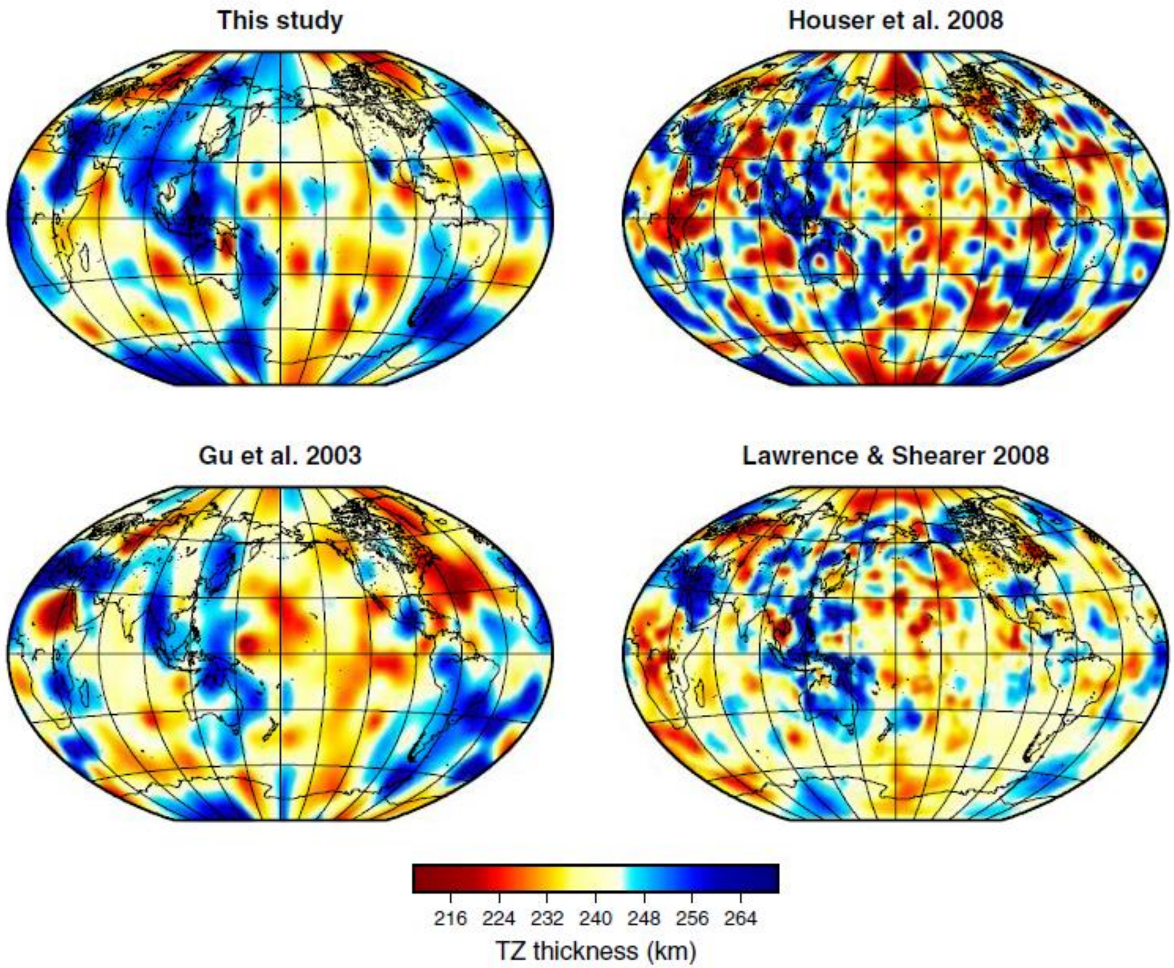

Fig. 10 Transition zone thickness measurements using SS precursors, comparing the results of different groups (this study; Gu et al. 2003; Houser et al. 2008; Lawrence and Shearer 2008). While the maps are quite different, some similarities can be found. A thickening of the transition zone can be seen in most maps, for example, in the Indonesian subduction zone region

after Deuss 2009

Thickness of interface

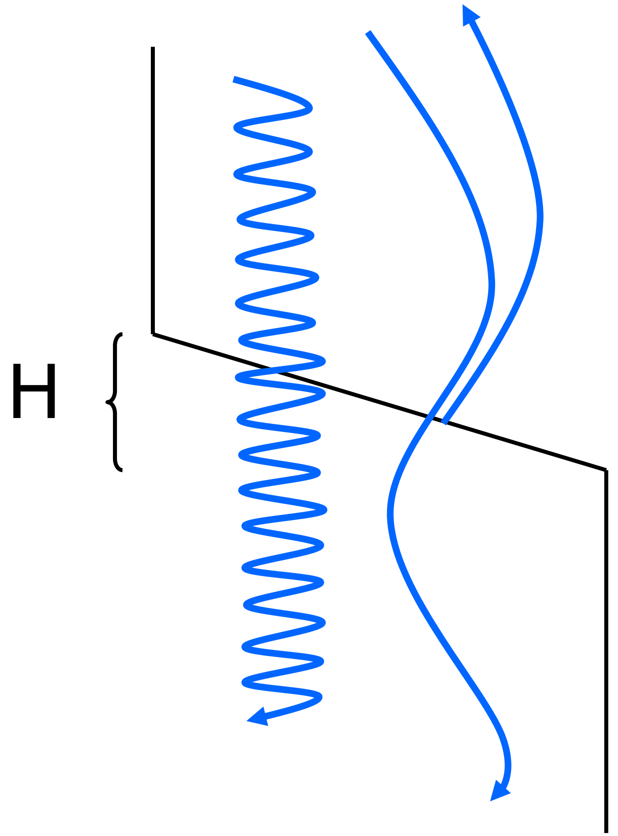

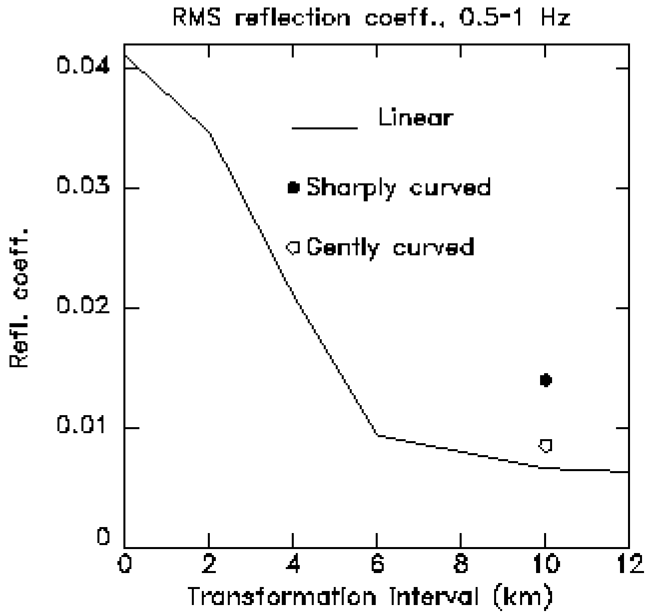

Thickness of 410-discontinuity from Helffrich and Wood, 1996:

around 4km

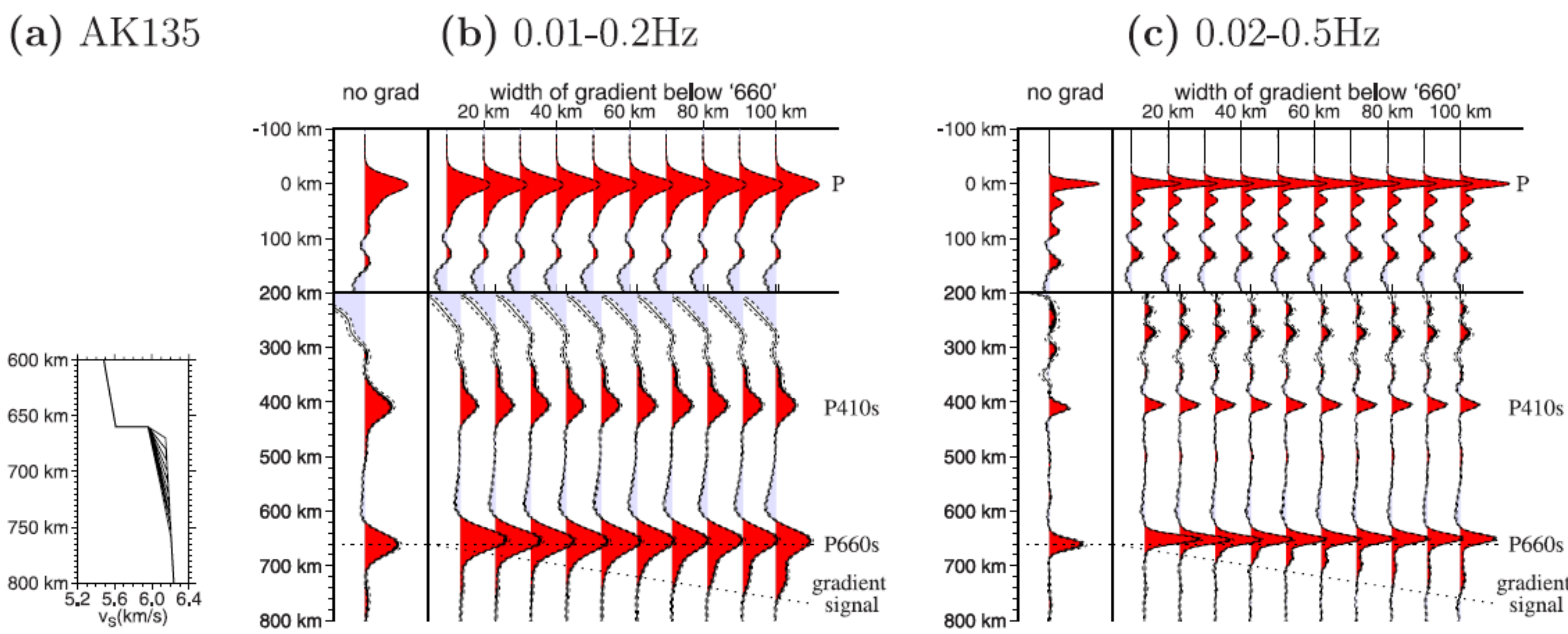

Figure 7. (a) The v_S profiles for models based on AK135 with modified structure beneath 660 km. (b) and (c) Stacked receiver functions for each model. Gradient width marked along the top axis refers to the enhanced gradient extending beneath the 660. The steep gradient affects the signals at 660 km depth. The main peak becomes broad and asymmetric as the gradient width increases, and in the higher-frequency band a distinct second maximum is generated. A different amplitude scale is used above and below 200 km.

after Andrews and Deuss 2008

UNIVERSITY OF OSLO

Summary on receiver functions

Unique to detect Moho, LAB, 410, 660 discontinuities

Advantages

- Constrain presence and depth of discontinuities
- Constrain sharpness of discontinuities to some extend
- Complementary to surface wave tomography

Disadvantages

- Coverage in regions with seismometers
- Give only velocity difference across jump